United States Department of Commerce
National Institute of Standards and Technology

NIST Technical Note 1554

Characterization of Tissue-Equivalent Materials for High-Frequency Applications (200 MHz to 20 GHz)

James Baker-Jarvis
Sung Kim
Luke E. Schallinger
Justin Johnson
Brad Givot

NIST Technical Note 1554

Characterization of Tissue-Equivalent Materials for High-Frequency Applications (200 MHz to 20 GHz)

†James Baker-Jarvis
†Sung Kim
‡Luke E. Schallinger
‡Justin Johnson
‡Brad Givot

†Electromagnetics Division, MS 818.01
National Institute of Standards and Technology
325 Broadway
Boulder, CO 80305-3337

‡3M Co
St. Paul, Minnesota

July 2010

U.S. Department of Commerce, Gary Locke, Secretary
National Institute of Standards and Technology, Patrick D. Gallagher, Director

National Institute of Standards and Technology Technical Note
Natl. Inst. Stand. Technol., Tech. Note 1554. 32 pages (July 2010)
CODEN:NTNOEF

U.S. GOVERNMENT PRINTING OFFICE
WASHINTON: 2010

For sale by the Superintendent of Documents, U.S. Government Printing Office, Washington, DC 20402-9325

Contents

Characterization of Tissue-Equivalent Materials for High-Frequency Applications (200 MHz to 20 GHz)

James Baker-Jarvis,* Sung Kim*

Luke E. Schallinger,† Justin Johnson,† and Brad Givot †

The purpose of this report is to summarize the characterization of a number of high-frequency solid, liquid, and semisolid tissue-equivalent materials, from 200 MHz to 20 GHz. Carbon black and liquid mixtures were studied, but were found to be unsuitable for matching both the real and imaginary parts of the permittivity over a broad range of frequencies. Agar and agarose-based materials produced stable materials whose real and imaginary parts of the permittivity exhibited the required dispersive characteristics and could be easily tuned to fit a specific application and over a given frequency range.

Key words: Agarose; carbon-black; dielectric; frequency; permittivity; phantom.

*National Institute of Standards and Technology, Electromagnetics Division, MS 818.01, Boulder, CO 80305

†3M Co., St. Paul, MN 55144-1001

1. Introduction

1.1 Overview of the Problem

Many research areas require electrical tests that use phantom materials with properties similar to that of the various tissues of the human body, over various frequency bands. In the past, tissue-equivalent materials have been used for applications that include studies on the low-frequency electromagnetic wave interaction with the human body, through-the-wall imaging, the interaction of medical implant devices, and the interaction of wireless transmitters with human tissue [1]. The conductivities and permittivities of the human body are highly inhomogeneous, and bone, blood, muscle, etc.; all have different permittivities and conductivities. Since the permittivity of human tissue is frequency dispersive, it is important that the simulant material mimics the frequency-dependent properties.

The interaction of biological tissues with electromagnetic waves is related to the conductivity and dielectric properties that are modeled through the permittivity $\varepsilon^*(\omega) = \varepsilon_0(\varepsilon_r'(\omega) - j(\sigma_{dc}/\varepsilon_0\omega + \varepsilon_r''(\omega))$, where $\varepsilon_0 \approx 8.854 \times 10^{-12}$ (F/m), ω is the radian frequency ($\omega = 2\pi f$), relative to the complex time dependence $\exp(j\omega t)$, $j = \sqrt{-1}$, and the dc conductivity is σ_{dc} (S/m). Since the real part of the permittivity is related to the impedance, it affects the reflectivity of an incident wave. The imaginary part of the permittivity relates to the wave attenuation as it passes into a material. The magnetic permeability of tissue-equivalent materials is very nearly that of free space, $\mu_0 = 4\pi \times 10^{-7}$ (H/m).

Various forms of tissue-equivalent materials have been studied by many researchers [2–14]. Previously developed phantom materials have been based on liquids and salts, gels, and carbon-black mixtures. For example, Hagmann et al. used glycine, salt, and the gelling agent, carrageenan [7]. With this mixture, they found they could match the permittivity and conductivities of the human body at lower frequencies. Materials that have dielectric properties similar to those of human tissue are most easily obtained by use of water-based mixtures. Usually the researcher requires materials that have time-stable properties. In addition, the materials must possess frequency-dispersive properties similar to human tissue. For this reason many different simulant materials have been developed over the years.

Kato et al [10] and Onishi et al. [4] used mixtures of agar, water, and salts. Kato found that the semi-solid material could be sculptured to produce a body shape, but it degraded in time. Chou et al. [8] used a mixture of water, salts, and a gelling agent to form a semi-solid material. A useful recipe for agar materials is given in [4]. Andreuccetti at al. [9] used a mixture of water, polyacrylamide, and salts to produce a semi-solid phantom. Marchal et al. [12] used a mixture of water, salts, and gelatine to produce a stable jelly-like phantom material. Addition of a preservative alleviates most of the time-stability problems. Most of the previous studies that dealt with low fre-

quencies used liquid materials, while the studies that dealt with megahertz to gigahertz frequencies used semi-solid materials [11]. Liquids work well as phantom materials for the dielectric loss at low frequencies because the mobile ions from the salts mimic the tissue's dielectric-loss response. However, the real part of the permittivity of most liquid phantoms is too high to match that of human tissue. The standard method for measuring the Specific Absorption Rate (SAR) caused by wireless communication devices uses a liquid mixture of water, NaCl, alcohol, sugar, and other additives, depending on the frequency [13]. The IEEE Standard uses a mixture of water, NaCl, sugar, and other compounds, as indicated in IEEE Standard Method 1528.

In our study the goal was to find materials that are time stable and easy to produce, and can be used from 200 MHz to 20 GHz. We considered carbon black mixed into silicone rubber (CBS), liquids, and agar and agarose-based composites mixed with powdered ethylene. Most of these composites can be mixed to match the average conductivity of the human body tissues, but the properties of the semi-solid materials most closely matched our criteria.

1.2 Electrical Properties of Tissue-Equivalent Materials

For a material that is homogeneous, linear and isotropic, the complex permittivity ε is defined by $\mathbf{D}(\omega) = \varepsilon(\omega)\mathbf{E}(\omega)$, where $\mathbf{E}$ is the complex time-harmonic, steady-state electric field intensity, and $\mathbf{D}$ is the corresponding displacement vector.

In conductive media, Maxwell's curl relation for the magnetic field intensity $\mathbf{H}$ is given by

$$\nabla \times \mathbf{H}(\omega) = j\omega\varepsilon_0\varepsilon_r'(\omega)\left[1 - j\left(\frac{\varepsilon_{r(d)}''(\omega)}{\varepsilon_r'(\omega)} + \frac{\sigma_{dc}}{\omega\varepsilon_0\varepsilon_r'(\omega)}\right)\right]\mathbf{E}(\omega). \tag{1}$$

We define the effective loss tangent as

$$\tan\delta_e(\omega) = \frac{\varepsilon_{r(d)}''(\omega)}{\varepsilon_r'(\omega)} + \frac{\sigma_{dc}}{\omega\varepsilon_0\varepsilon_r'(\omega)}. \tag{2}$$

The two terms in Eq.(2) represent different effects that are responsible for the conductive loss in a material. We identify these terms in the following manner. The frictional losses due to dipole movement are related to

$$\tan\delta_d(\omega) = \frac{\varepsilon_{r(d)}''(\omega)}{\varepsilon_r'(\omega)}, \tag{3}$$

and the dc conduction losses are modeled as

$$\tan\delta_m(\omega) = \frac{\sigma_{dc}}{\omega\varepsilon_0\varepsilon_r'(\omega)}. \tag{4}$$

The term $\tan\delta_d$ represents losses in materials classified as dielectrics or insulators where there are essentially no free charge carriers. At the other extreme, $\tan\delta_m$ dominates in highly conductive

liquids and metals. The complex permittivity including the conductivity is defined as

$$\varepsilon^* = \varepsilon_r'\varepsilon_0 - j(\varepsilon_r''\varepsilon_0 + \frac{\sigma_{dc}}{\omega}). \tag{5}$$

The conductivity σ_{dc} is nearly independent of frequency in the rf and microwave bands, but $\sigma_{eff} = \varepsilon_0\omega\varepsilon_r''$ increases nearly linearly for many lossy solids and semisolids.

Fields attenuate as they enter materials that have loss and can be modeled as a damped exponential $E(x) = E_0\exp(-x/\delta_s)$. The skin depth δ_s is the distance a plane wave travels until its magnitude decreases by $1/e$ and is defined for lossy dielectric materials as

$$\delta_s = \frac{\sqrt{2}c}{\omega}\frac{1}{\sqrt{\varepsilon_r'\mu_r'}\sqrt{\sqrt{1+\tan^2\delta_d}-1}}. \tag{6}$$

In Eq.(6) δ_s reduces in the low conductivity limit to $\delta_s \rightarrow 2c\sqrt{\varepsilon_r'}/\omega\sqrt{\mu_r'}\varepsilon_r''$. Tissues have medium to high loss so it is better to use the exact equation Eq. (6) to calculate skin depth. From Eq.(6), we see that the frequency, permittivity, and permeability of the material determine the skin depth. The higher the frequency, permeability, and conductivity, the shorter the skin depth [15]. The depth of penetration $D_p = \delta_s/2$ is the depth where the energy in the wave drops to $1/e$ of its value on the surface. The skin depth in human tissues is on the order of 5 cm at 500 MHz to 1 cm at 5 GHz. Gabriel and Gestblom have compiled extensive data on various human tissues and developed a database that reports measurements of various human tissues such as head, brain, muscle, fat, and bone [16].

The wavelength of an electromagnetic wave in a material is influenced by the permittivity: $\lambda \approx c_{vac}/\sqrt{\varepsilon_r'\mu_r}f$, where c_{vac} is the speed of light in vacuum. The impedance is a strong function of σ_{dc} at low frequencies. For TEM waves, the plane-wave impedance is $Z = \sqrt{\mu^*/\varepsilon^*} = \sqrt{j\omega\mu'/(j\omega\varepsilon' + \sigma_{dc})}$ and $Z_0 = \sqrt{\mu_0/\varepsilon_0}$ is the impedance of free space; the plane-wave reflection coefficient is given by

$$\Gamma_p = \frac{Z - Z_0}{Z + Z_0}. \tag{7}$$

Most conductive semisolid materials have an effective conductivity that is relatively constant below 100 MHz and then increases with frequency above 100 MHz. This indicates that dc conduction dominates at low frequencies, but as the frequency increases the dielectric loss also contributes.

2. Previous Research on the Dielectric Properties of Human Tissue

Schwan, Foster, Stuchly, Gabriel [2, 17, 18], and others performed studies on dielectric properties of human tissues. Gabriel's results are summarized in a database [18, 19]. Typical results are

displayed in Figs. 1, 2, and 3. Note the behavior of the conductivity from low frequency to 20 GHz. Below 200 MHz the conductivity is relatively flat, but it increases almost linearly at higher frequencies up to about 20 GHz and then the slope decreases. This is due to the transition from dc conductivity to dielectric relaxation. The body is a complicated mixture of organs and materials with widely varying dielectric properties, and so choosing an effective material that matches the average body properties as a function of frequency is difficult and only approximate.

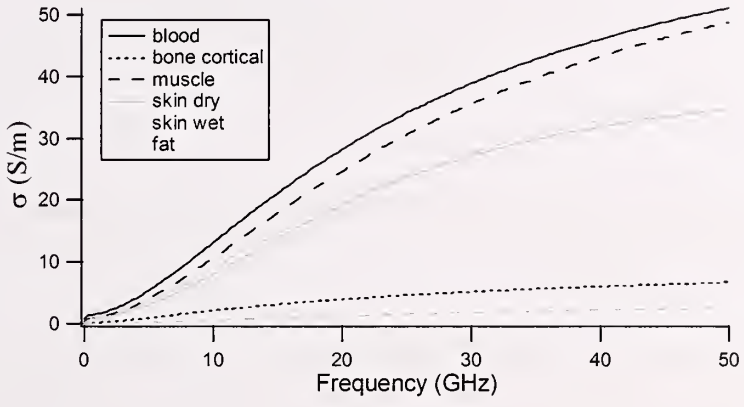

Figure 1. Measurements of the conductivity (S/m) of various body tissues by Gabriel and Gestblom [16] (no uncertainties assigned).

In Fig. 4 we display the skin depth of human skin as a function of frequency. We see that even at 10 GHz the wave penetrates around 4 mm into the skin layer and into the muscle and bone. At 100 MHz the skin depth is nearly the thickness of the body. As a consequence, simulating human body properties by spray-on paints or thin veneers on a manikin may work for a specific frequency, but will fail over a broad band of frequencies.

3. Dielectric Measurement Methods for Tissue-Equivalent Materials

Over the years, there has been an abundance of methods developed for measuring the complex permeability and permittivity of lossy materials. These techniques include free-space methods, open-ended coaxial-probes, cavity resonators, dielectric-resonator techniques, and transmission-line techniques [20]. Each dielectric measurement method has a niche. For example, techniques

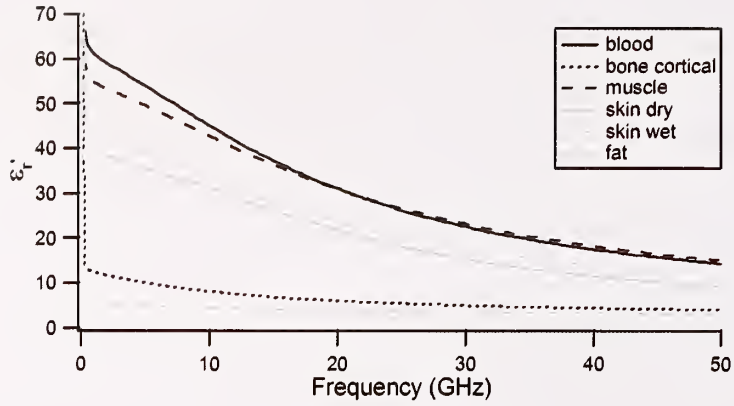

Figure 2. Measurements of the relative permittivity of various body tissues by Gabriel and Gestblom [16] (no uncertainties assigned).

based on cavities are accurate, but not broadband, and are usually limited to low-loss materials. Nondestructive techniques, although not the most accurate, are very attractive because they maintain the integrity of the material. Tissue-equivalent materials are lossy, and consequently resonance methods are difficult to use. Therefore the researcher must use a transmission-line method of some type. For semi-solid materials, open-ended coaxial probes, as shown in Fig. 5, are easy to apply. We used coaxial probes with apertures from 3.5 mm to 14 mm for most of the measurements in this report. However, the ε_r' measured by coaxial probes are influenced by air gaps between the material under test and the fixture. This air gap influence is less severe for semisolid materials than for solid materials. As a check on our probe operation we commonly measure standard liquids. In Fig. 6 the real and imaginary parts of methanol are plotted for measurements with a 14 mm probe. As another test, we measured ham as a function of frequency because it has properties similar to human tissue, but, is of course not a standard material (see Figs. 7 and 8). The uncertainty analysis we used for the coaxial probe measurements was based on the analysis given in Ref. [21] that uses the root-mean square (RMS) method.

3.1 Solid Simulants

For use as a candidate tissue-equivalent material we developed a carbon black silicone composite in collaboration with 3M Co. and Dyneon, Inc. Measured data for this material are shown in Figs. 9 and 10. These materials can be made so that the ε_r' and dispersive characteristics approximately

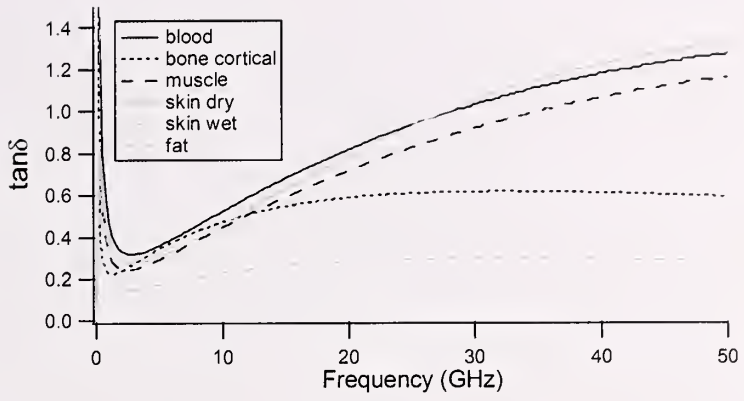

Figure 3. Measurements of the loss tangent of various body tissues by Gabriel and Gestblom [16] (no uncertainties assigned).

match those of human body tissues. However, we cannot design these materials to match simultaneously both ε_r' and ε_r''. In Fig. 11, we show how the conductivity of carbon black in a polymer base varies as a function of the carbon black concentration from 1 kHz to 1 MHz. In addition, these materials are difficult to manufacture reproducibly. For the carbon black composite, the Type B expanded relative uncertainty for ε_r', $U = ku_c = 3.0$ (k=2). We have observed that obtaining highly repeatable measurements on carbon-black composites is difficult. This is due to the heterogeneity of the material. In order to understand the various measurement issues in measuring carbon-black composite materials we participated in an intercomparison with the National Physical Laboratory of UK (NPL) and a number of industrial partners. The material was a mixture of graphite and polymer. Each group in the study received samples of the materials from the same manufacturer and measured the materials with their in-house methods. Because each participant's material was from a different batch, any manufacturing inhomogeneities or batch-to-batch variations influenced the measurements. The results of these measurements are given in Figs. 12 and 13. This intercomparison shows that measurements on these artificial materials generally have large systematic uncertainties associated with them that are due to inhomogeneities and the effects of air gaps.

3.2 Liquid Simulants

Solutions of water mixed with salts can be developed that exhibit the appropriate conductivity in the microwave range. However, the proper values for ε_r' are difficult to obtain. In Fig. 14, the dc

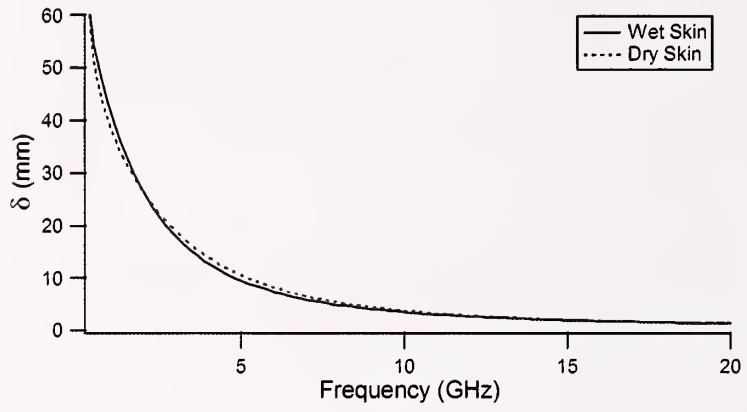

Figure 4. The calculated skin depth in millimeters from the skin data of Gabriel and Gestblom [16].

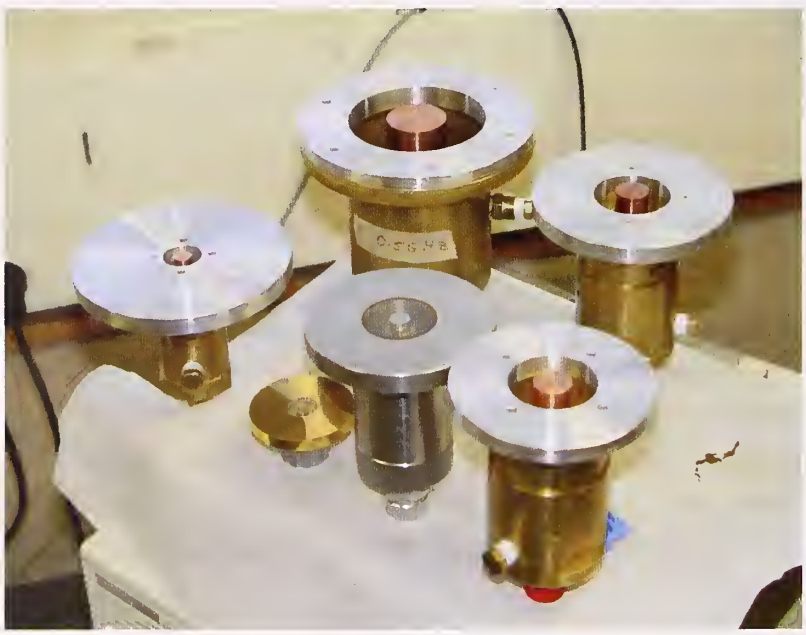

Figure 5. Some of the open-ended coaxial probes used in this research

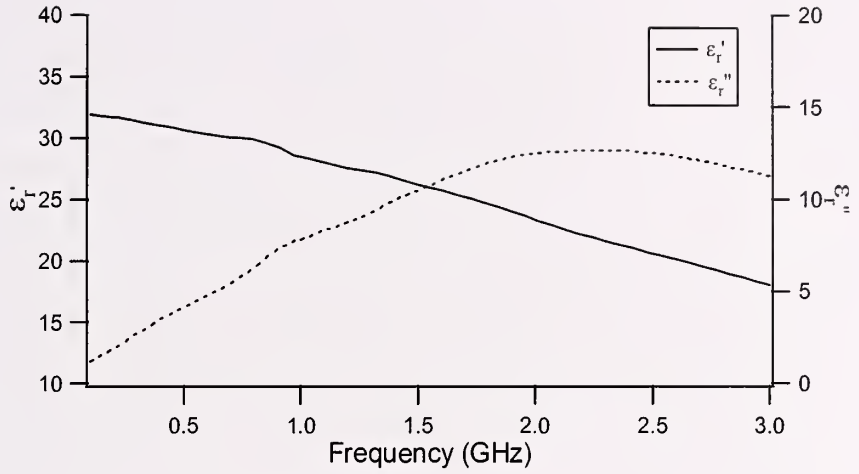

Figure 6. Measurements of ε_r' and ε_r'' for methanol at 20^{o}C by use of a 14 mm open-ended coaxial probe. For measured ε_r', the Type B expanded relative uncertainty was $U = ku_c = 1.5$ (k=2), where k is coverage factor.

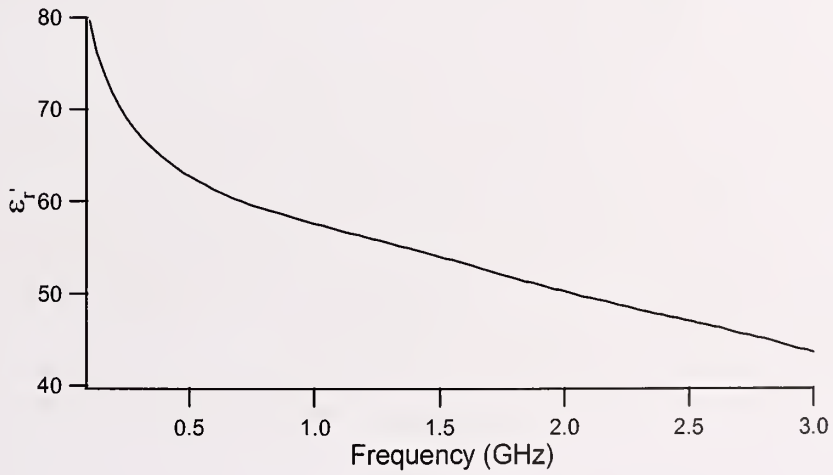

Figure 7. The real part of the permittivity of cooked, processed ham as a function of frequency.

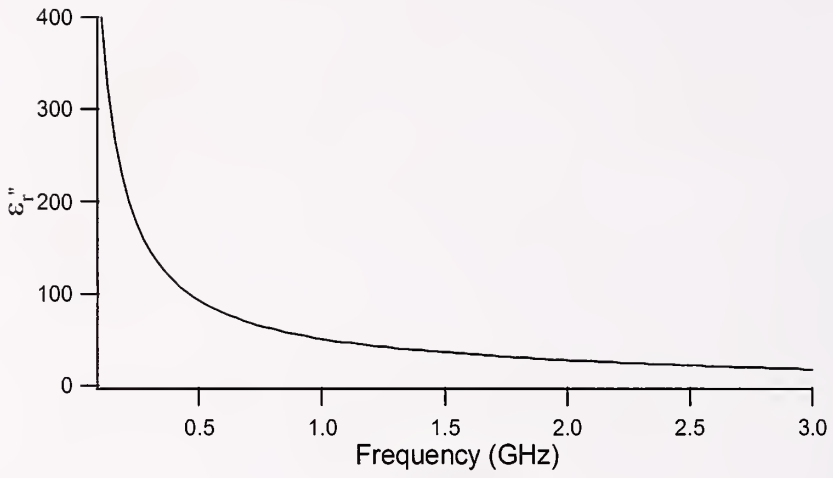

Figure 8. The loss factor of cooked, processed ham as a function of frequency.

conductivity of potassium chloride water solutions (KCl) in 500 ml deionized water is plotted for various concentrations of salts. The uncertainties in the liquid measurement are due to uncertainties in the measurement device and uncertainties in the chamber temperature. Measurements in our lab have a temperature stability of $\pm 2\ ^{o}$C.

The conductivities of liquids that contain free ions from salts are approximately independent of frequency. This is in contrast to tissues, where the conductivity increases for frequencies above 100 MHz. This is probably due to interfaces in the materials.

We also measured another liquid mixture that contained a 50-50 mix of ethylene carbonate-propylene carbonate with the salt tetraethyleammonium tetrafluoroborate (TEATFB) developed by Broadhurst et al. [5]. Measured data are shown in Fig. 15. We found that by varying the salt concentration we could vary the conductivity over the desired range found in human tissues. The following formula as derived from Fig. 14 approximates the conductivity data as a function of grams of TEATFB (m_{tea}) per 100 g of propylene carbonate:

$$\sigma = 0.0095 + .0725 m_{tea} - 0.00112 m_{tea}^2. \tag{8}$$

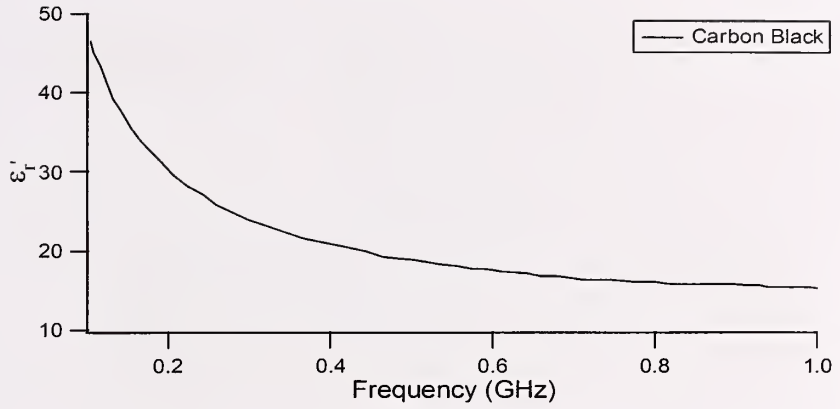

Figure 9. The permittivity of a polymer carbon black composite.

3.3 Agar and Agarose-Based Tissue-Equivalent Materials

Although the conductivities of human tissues can be simulated by conducting liquids, the real part of the permittivities of these liquids does not match that of human tissue. In order to find a better material, we have developed agar and agarose-based materials, as shown in Fig. 16, which shows a simulant human hand. Agarose is polysaccharide obtained from agar that is the most widely used medium for gel electrophoresis tests. We found that we could vary both the conductivity, dispersion, and the real part of the permittivity by changing the proportions of the constituents. The conductivity was varied by changing the amount of potassium chloride phosphate buffered saline (PBS) included. The real part of the permittivity was varied by adding polyethylene powder. A preservative is usually added to prevent agar decomposition. In Figs. 17 and 18 we present the real and imaginary parts of permittivity measurements for agar composites, without polyethylene, from 500 MHz to 20 GHz as measured with a 3.5 mm open-ended coaxial probe. Figs. 19 and 20 show results of measurements with a 14 mm coaxial probe from 100 MHz to 2 GHz on an agarose material with added polyethylene powder. Figs. 21 through 24 show measurements on another mixture of agarose through the use of 14 mm and 3.5 mm probes. These results are compared to a mixture with 7 % by weight of polyethylene. For agar mixture recipes see Onishi et al. [4].

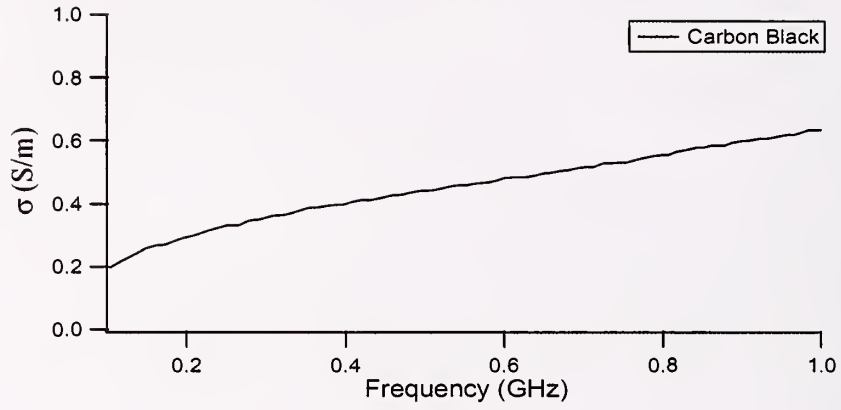

Figure 10. The conductivity of a polymer carbon black composite.

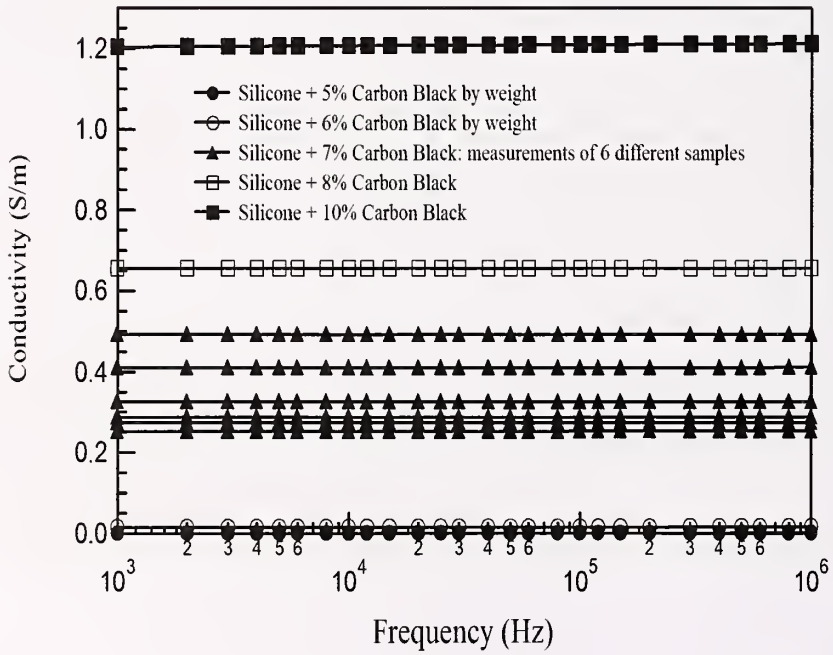

Figure 11. The conductivity of silicone as a function of added carbon black and frequency.

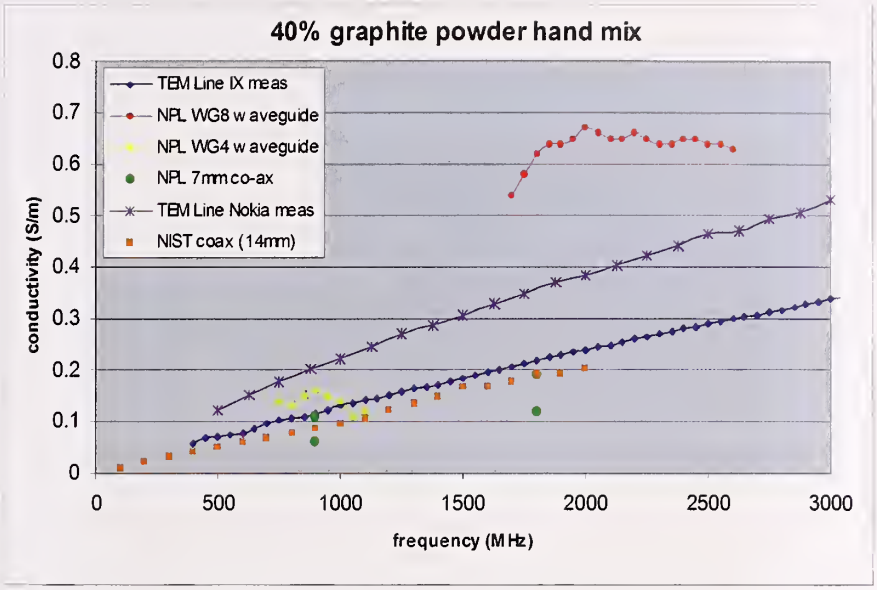

Figure 12. The round-robin measurement results for the conductivity of a graphite-polymer composite.

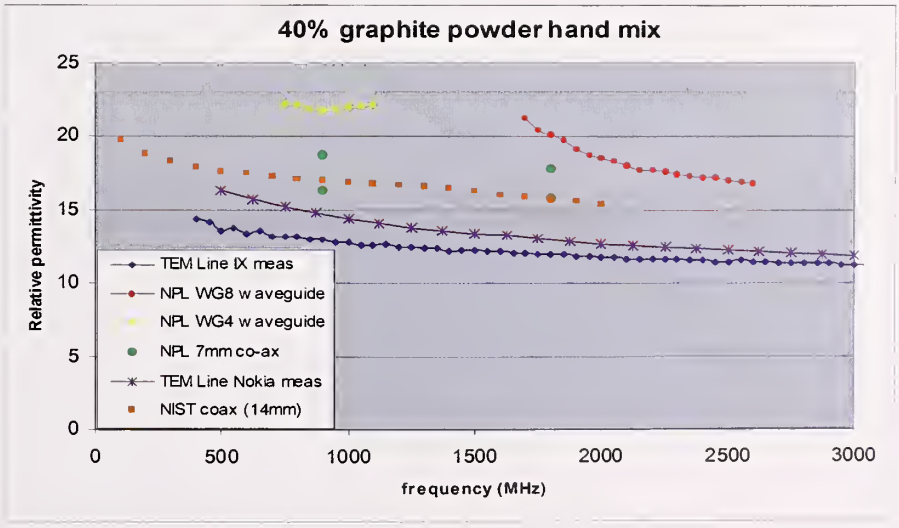

Figure 13. The round-robin measurement results for ε_r' of the graphite-polymer composite.

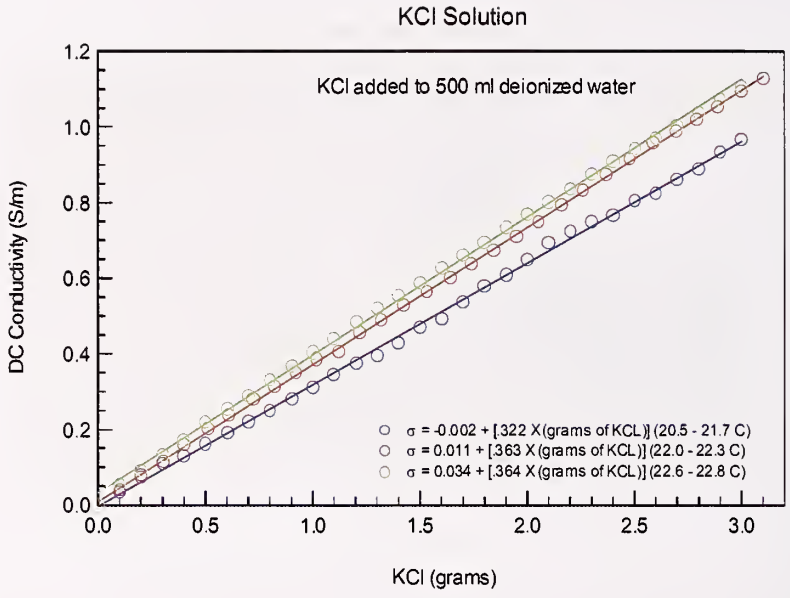

Figure 14. Conductivity of KCl solution versus concentration and temperature.

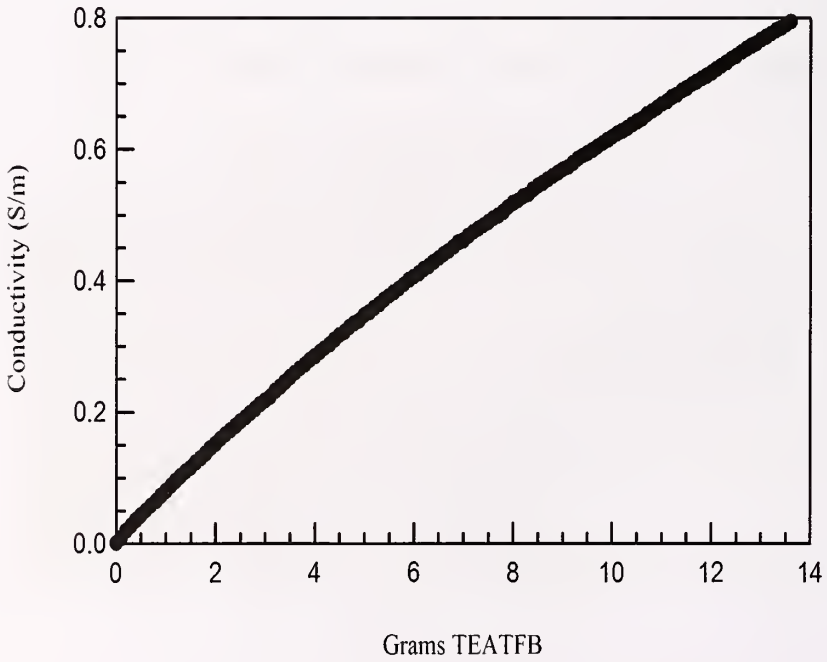

Figure 15. The dc conductivity of the TEATFB solution containing 100 ml propylene carbonate and 125 g ethylene carbonate as a function of TEATFB concentration.

Figure 16. Phantom hand made from a glove filled with agarose

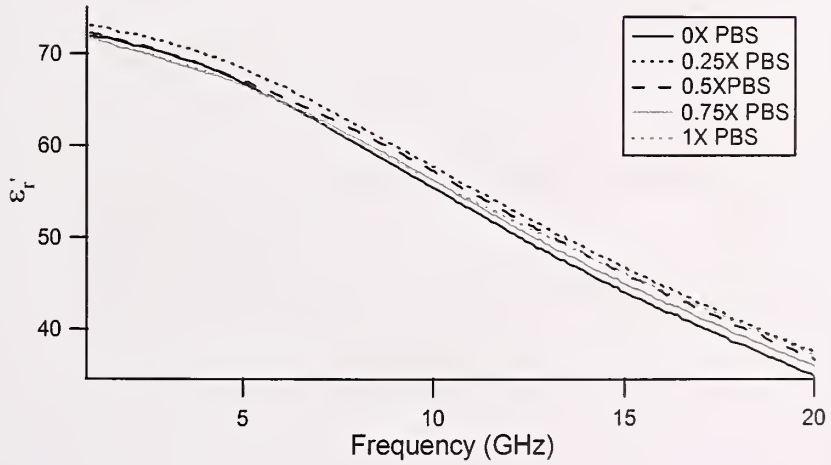

Figure 17. Real part of the permittivity of an agarose-based material as a function of frequency.

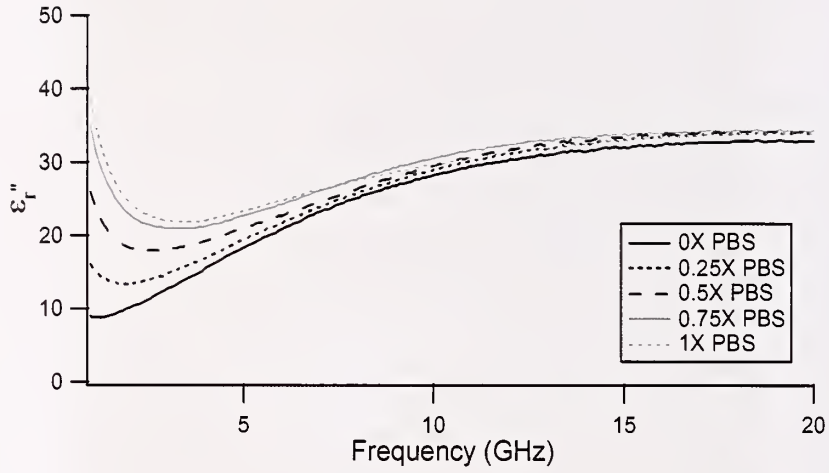

Figure 18. Loss factor of an agarose-based material as a function of frequency.

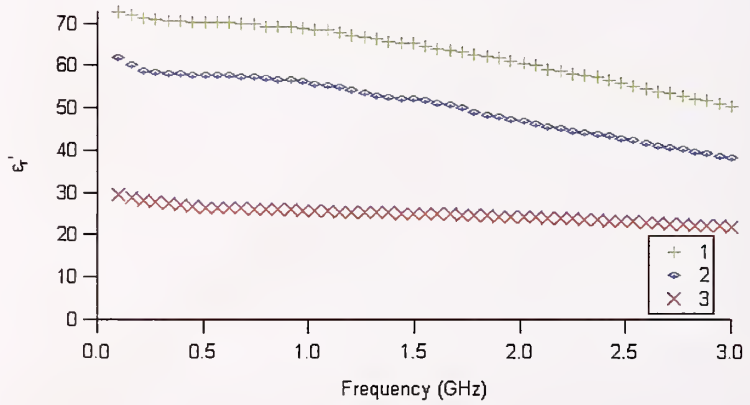

Figure 19. ε_r' of agarose mixed with polystyrene powder as measured with a 14 mm coaxial probe. The top curve is for agarose with no polyethylene powder, and the lower curves are for 15 % and 25 % polyethylene powder added.

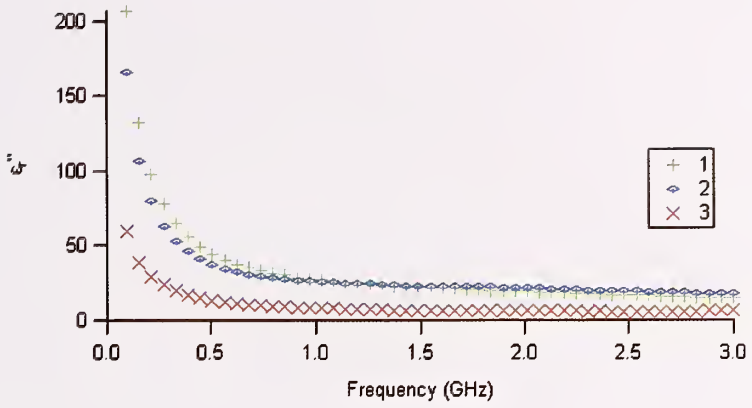

Figure 20. Loss factor of agarose mixed with polystyrene powder as measured with a 14 mm coaxial probe. The top curve is agarose with no polyethylene powder and the lower curves are with 15 % and 25 % polyethylene powder included.

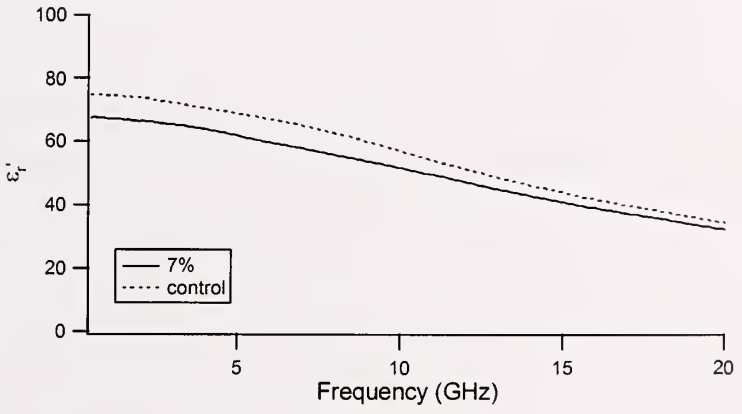

Figure 21. The real part of the permittivity for agarose-based specimens measured from 500 MHz to 20 GHz with a 3.5 mm coaxial probe. The top curve is agarose with no polyethylene powder added and the lower one is for agarose with 7 % polyethylene powder added.

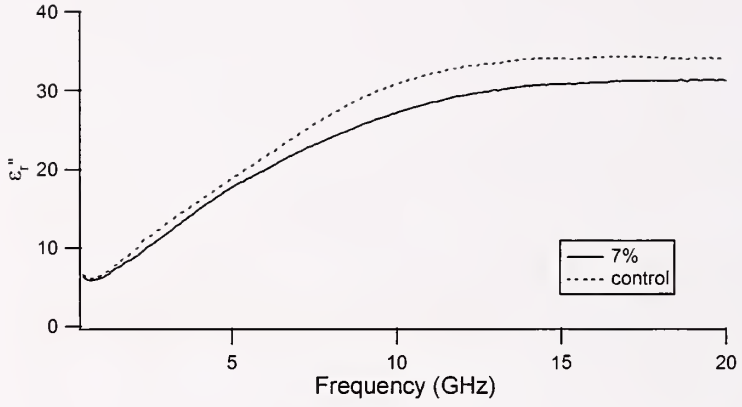

Figure 22. The loss factor for agarose-based specimens measured from 500 MHz to 20 GHz with a 3.5 mm coaxial probe. The top curve is for agarose with no polyethylene powder added and the lower one with 7 % polyethylene powder added.

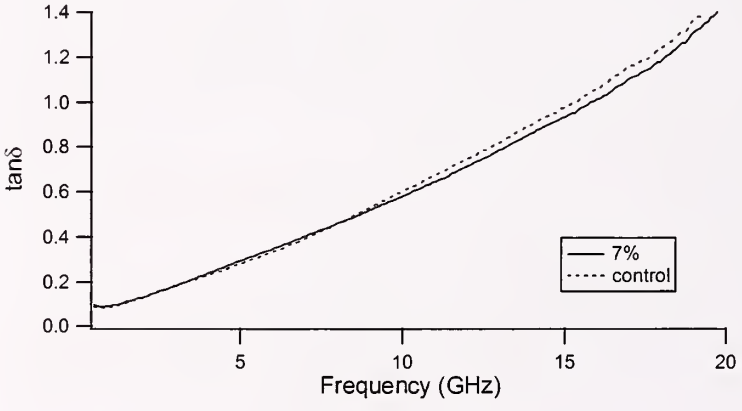

Figure 23. The loss tangent for agarose-based specimens measured from 500 MHz to 20 GHz with a 3.5 mm coaxial probe. The top curve is for agarose with no polyethylene powder, and the lower one is with polyethylene powder.

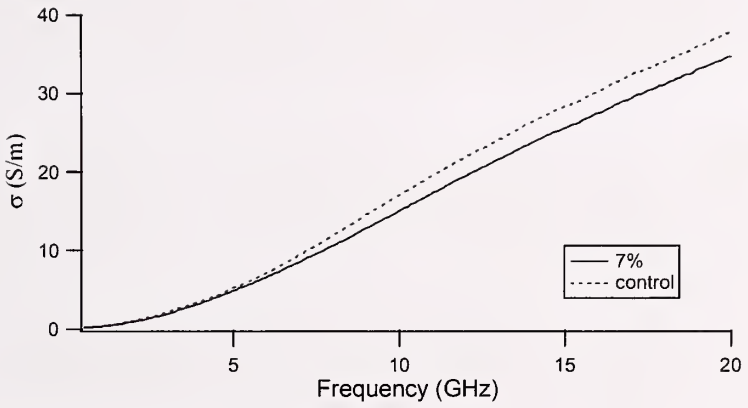

Figure 24. The conductivity for agarose-based specimens measured from 500 MHz to 20 GHz with a 3.5 mm coaxial probe. The top curve is for agarose with no polyethylene powder added and the lower one is for agarose with polyethylene powder added.

4. Discussion

We have shown that conductivities with a few percent of those of tissues in the human body can be reproduced by either solid carbon-black composites, various conducting solutions, or semi-solid agarose-based materials. The real part of the permittivity can most easily be produced by agar and agarose-based materials with polyethylene powder added. The liquids can easily be mixed to obtain the desired response. These liquids also show good time stability. We found that as the fraction of polyethylene powder was increased above 15 % by weight the structural integrity of the material was degraded.

We acknowledge the support of Office of Law Enforcement Standards (OLES) at NIST and the National Institute of Justice and discussions with Nick Paulter of the of OLES.

5. References

[1] K. L. Stricklett and J. Baker-Jarvis, *Electrical Properties of Biological Materials: A Bibliographic Survey*. 2001. NIST IR 6564.

[2] K. R. Foster and H. P. Schwan, *Dielectric properties of tissues and biological materials: A critical review*, vol. 17, pp. 25–104. CRC Press, 1989.

[3] O. Martinsen, S. Grimmes, and H. Schwan, "Interface phenomena and dielectric properties of biological tissues," *Encyclopedia of Surface and Colloid Science*, p. 2643, 2002.

[4] T. Onishi, R. Ishido, T. Takimoto, K. Saito, S. Uebayashi, M. Takahashi, and K. Ito, "Biological tissue-equivalent agar-based solid phantoms and SAR estimation using thermographic method in the range of 3-6 GHz," *IEICE Trans. Commun.*, vol. E88-B, pp. 3733–3740, 2005.

[5] M. G. Broadhurst, C. K. Chiang, and G. T. Davis, "Dielectric phantoms for electromagnetic radiation," *J. Mole. Solids*, vol. 36, pp. 47–64, 1987.

[6] T. Kobayashi, T. Nojima, K. Yamada, and S. Uebayashi, "Dry phantom composed of ceramics and its application to SAR estimation," *IEEE Trans. Microwave Theory Tech.*, vol. 41, pp. 136–140, 1993.

[7] M. J. Hagmann, R. Calloway, A. Osborn, and K. Foster, "Muscle equivalent phantom materials for 10-100 MHz," *IEEE Trans. Microwave Theory Tech.*, vol. 40, pp. 760–762, 1992.

[8] C. Chou, G. Chen, A. Guy, and K. Luk, "Formulas for preparing phantom muscle tissue for various radiofrequencies," *Bioelectromagn.*, vol. 5, pp. 435–441, 1984.

[9] D. Andreuccetti, M. Bini, and A. Ignesti, "Use of polyacrylamide as a tissue-equivalent material in the microwave range," *IEEE Trans. Biomed. Eng.*, vol. 35, pp. 275–277, 1988.

[10] H. Kato and T. Ishida, "Development of an agar phantom adaptable for simulation of various tissues in the range 5-40 MHz," *Phys. Med. Bio.*, vol. 32, pp. 221–226, 1987.

[11] Y. Nikawa, M. Chino, and K. Kikuchi, "Soft and dry phantom modeling material using silicone rubber with carbon fiber," *IEEE Trans. Microwave Theory Tech.*, vol. 44, pp. 1949–1953, 1996.

[12] C. Marchal, M. Nadi, A. J. Tosser, C. Roussey, and M. L. Gaulard, "Dielectric properties of gelatine phantoms used for simulations of biological tissues between 10 and 50 MHz," *Int. I. Hyperthermia*, vol. 5, no. 6, pp. 725–732, 1989.

[13] "Cenelec standard 50361: Basic standard for the measurement of the specific absorption rate related to human exposure to electromagnetic fields from mobile phones (300 MHz - 3 GHz)," *CENELEC*, 2000.

[14] P. S. Hall and Y. Hao, *Antennas and propagation for body-centric wireless communications*. Boston: Artech House, 2006.

[15] M. J. Peters, J. G. Stinstra, and M. Hendriks, "Estimation of the electrical conductivity of human tissue," *Electromagn.*, vol. 21, pp. 545–557, 2001.

[16] C. Gabriel and B. Gestblom, "Microwave absorption in aqueous solutions," *Nature*, vol. 328, pp. 145–146, 1987.

[17] M. A. Stuchly and S. S. Stuchly, "Coaxial line reflection methods for measuring dielectric properties of biological substances at radio and microwave frequencies-A review," *IEEE Trans. Instrum. Meas.*, vol. IM-29, pp. 176–183, 1980.

[18] C. Gabriel, "Compilation of the dielectric properties of body tissues at RF and microwave frequencies," Tech. Rep. AL/OE-TR-1996-0037, Brooks Air Force Base, 1996.

[19] C. Gabriel, S. Gabriel, and E. Corthout, "The dielectric properties of biological tissues: I. Literature survey," *Phys. Med. Biol.*, vol. 41, pp. 2231–2249, 1996.

[20] J. Baker-Jarvis, M. D. Janezic, B. Riddle, C. L. Holloway, N. G. Paulter, and J. E. Blendell, *Dielectric and conductor-loss characterization and measurements on electronic packaging materials.* July 2001. NIST Tech. Note 1520.

[21] J. Baker-Jarvis, M. D. Janezic, J. H. Grosvenor, and R. G. Geyer, *Transmission/Reflection and Short-Circuit Line Methods for Measuring Permittivity and Permeability.* 1992. NIST Tech. Note 1355.

A. Appendix: Fundamental Electromagnetic Parameters and Concepts Used in Material Characterization

In this section, we review the most basic concepts needed to study and interpret dielectric and magnetic response in materials. For anisotropic and gyrotropic media the most general forms of the permittivity and permeability are

$$\overleftrightarrow{\varepsilon}(\omega) = \begin{pmatrix} \varepsilon_x & -j\kappa_e & 0 \\ j\kappa_e & \varepsilon_y & 0 \\ 0 & 0 & \varepsilon_z \end{pmatrix}, \tag{9}$$

$$\overleftrightarrow{\mu}(\omega) = \begin{pmatrix} \mu_x & j\kappa_m & 0 \\ -j\kappa_m & \mu_y & 0 \\ 0 & 0 & \mu_z \end{pmatrix}. \tag{10}$$

The off-diagonal elements are due to gyrotropic behavior in an applied magnetic field.

In the time domain, material response can be obtained by analyzing the response to a pulse or impulse. The most general causal linear relationship between the displacement and electric fields is

$$\mathbf{D}(\mathbf{r},t) = \varepsilon_0 \mathbf{E}(\mathbf{r},t) + \int_0^\infty \overleftrightarrow{f}(\tau) \cdot \mathbf{E}(\mathbf{r},t-\tau)d\tau, \tag{11}$$

where $\overleftrightarrow{f}$ is the impulse-response function and $\mathbf{D} = \varepsilon_0\mathbf{E} + \mathbf{P}$. The permittivity is defined in terms of the Fourier transform of the impulse-response function, $\varepsilon(\omega) = \varepsilon_o(1 + \mathcal{F}[\overleftrightarrow{f}](\omega))$. An analogous equation can be written between the induction and magnetic fields. From Eq. (11), for isotropic linear media, $\varepsilon_r^*(\omega) = \varepsilon_{r\infty} + \chi_r(\omega) = \varepsilon_r'(\omega) - j\varepsilon_r''(\omega)$, ($\varepsilon_{r\infty}$ is the relative optical-limit of the relative permittivity.

Electric and magnetic fields are attenuated as they travel through lossy materials. The plane-wave attenuation coefficient in an infinite medium is denoted by the quantity α and the phase by β. The propagation coefficient is $\gamma = \alpha + j\beta = jk \rightarrow j\omega\sqrt{\varepsilon\mu}$. For waves in a guided structure, $\gamma =$

$j\sqrt{k^2-k_c^2}$, where $k_c = \omega_c/c = 2\pi/\lambda_c$ is the cutoff wave number, with $k = \omega\sqrt{\varepsilon'\mu'}/c$. Attenuation is given by

$$\alpha = \frac{\omega}{\sqrt{2}c}\sqrt{\varepsilon'_r\mu'_r}\sqrt{((\tan\delta_d\tan\delta_m - 1)^2 + (\tan\delta_d + \tan\delta_m)^2)^{1/2} + \tan\delta_d\tan\delta_m - 1}. \tag{12}$$

We approximate this for dielectric materials as

$$\alpha = \frac{\omega}{\sqrt{2}c}\sqrt{\varepsilon'_r\mu'_r}\sqrt{\sqrt{1+\tan^2\delta_d} - 1}. \tag{13}$$

For energy considerations α must always be positive. In low-loss dielectric media, $\tan_d\delta \ll 1$ and α reduces in the limit to $\alpha \to \omega\sqrt{\varepsilon'_r\mu'_r}\tan\delta_d/2c$. The phase coefficient β is given by

$$\beta = \pm\frac{\omega}{\sqrt{2}c}\sqrt{\varepsilon'_r\mu'_r}\sqrt{((\tan\delta_d\tan\delta_m - 1)^2 + (\tan\delta_d + \tan\delta_m)^2)^{1/2} - (\tan\delta_d\tan\delta_m - 1)}. \tag{14}$$

Note that at cutoff, β is a function only of the loss factors. In dielectric media β reduces to

$$\beta = \pm\frac{\omega}{\sqrt{2}c}\sqrt{\varepsilon'_r\mu'_r}\sqrt{\sqrt{1+\tan^2\delta_d} + 1}. \tag{15}$$

The imaginary part of the propagation coefficient defines the phase of an electromagnetic wave and is related to the refractive index $n = \pm\sqrt{\varepsilon'_r\mu'_r}$. In normal dielectrics the positive square root is taken in Eq. (14). The wave impedance for a transverse electric and magnetic mode (TEM) is $\sqrt{\mu/\varepsilon}$; for a transverse electric mode (TE) is $j\omega\mu/\gamma$; and for a transverse magnetic mode (TM) is $\gamma/j\omega\varepsilon$. As a consequence of conservation of energy, α must be positive. Below cutoff the propagation coefficient becomes $\gamma = \sqrt{k_c^2 - k^2}$, because a factor of j is factored out from under the square root.

The wavelength in a material is influenced by the permittivity; for example, for a TEM mode, $\lambda_m \approx c_{vac}/\sqrt{\varepsilon'_r\mu'_r}f$.

The skin depth, the distance a plane wave travels such that its amplitude decays to $1/e$ of its initial amplitude, is related to the attenuation coefficient by $\delta_s = 1/\alpha$. Due to losses, the wave amplitude decays as $|\mathbf{E}| \propto \exp(-\alpha z)$. The power in a plane wave, $E(z,t) = E_0\exp(-\alpha z)\exp(j(\omega t - \beta z))$, attenuates as $P \propto \exp(-2\alpha z)$. The surface impedance in ohms of a conducting material is $Z_m = (1+j)\sigma\delta_s$. In metals, where the conductivity is large, the skin depth reduces to

$$\delta_s = \frac{1}{\sqrt{\pi f\mu_0\mu'_r\sigma_{dc}}}, \tag{16}$$

where σ_{dc} is the dc conductivity and f is the frequency. We see that the frequency, conductivity, and permeability of the material determine the skin depth in metals. The surface resistance for

highly lossy materials is

$$R_s = \frac{1}{\delta_s \sigma_{dc}} = \sqrt{\frac{\pi f \mu_0 \mu_r'}{\sigma_{dc}}}. \tag{17}$$

When the conductors on a substrate are very thin, the fields can penetrate through the conductors into the substrate. This increases the resistance because the field is in both the metal and the dielectric. As a consequence of the skin depth, the internal inductance decreases with increasing frequency, whereas the surface resistance R_s of many metals increases with frequency in proportion to $\sqrt{f}$.

Some materials exhibit ionic conductivity, so that when a static (dc) electric field is applied, a current is induced. This behavior is modeled by the dc conductivity σ_{dc}, which produces a low-frequency loss ($\propto 1/\omega$) in addition to polarization loss (ε_r''). In some materials, such as semiconductors and disordered solids, the conductivity is complex and depends on frequency. This is because the free charge is partially bound and moves by tunneling through potential wells or hops from well to well.

The complex power flux is summarized by the complex Poynting vector $\mathbf{S}_c = (1/2)(\mathbf{E}(\mathbf{r},\omega) \times \mathbf{H}^*(\mathbf{r},\omega))$. The real part of $\mathbf{S}_c$ represents dissipation and is the time average over a complete cycle of the time-domain Poynting vector $\mathbf{S}(\mathbf{r},t) = \mathbf{E}(\mathbf{r},t) \times \mathbf{H}(\mathbf{r},t)$. The imaginary part of $\mathbf{S}_c$ relates to the difference between the electric and magnetic stored energy, and when averaged over one cycle it vanishes.

NIST Technical Publications

Periodical

Journal of Research of the National Institute of Standards and Technology–Reports NIST research and development in metrology and related fields of physical science, engineering, applied mathematics, statistics, biotechnology, and information technology. Papers cover a broad range of subjects, with major emphasis on measurement methodology and the basic technology underlying standardization. Also included from time to time are survey articles on topics closely related to the Institute's technical and scientific programs. Issued six times a year.

Nonperiodicals

Monographs–Major contributions to the technical literature on various subjects related to the Institute's scientific and technical activities.
Handbooks–Recommended codes of engineering and industrial practice (including safety codes) developed in cooperation with interested industries, professional organizations, and regulatory bodies.
Special Publications–Include proceedings of conferences sponsored by NIST, NIST annual reports, and other special publications appropriate to this grouping such as wall charts, pocket cards, and bibliographies.
National Standard Reference Data Series–Provides quantitative data on the physical and chemical properties of materials, compiled from the world's literature and critically evaluated. Developed under a worldwide program coordinated by NIST under the authority of the National Standard Data Act (Public Law 90-396). NOTE: The Journal of Physical and Chemical Reference Data (JPCRD) is published bimonthly for NIST by the American Institute of Physics (AIP). Subscription orders and renewals are available from AIP, P.O. Box 503284, St. Louis, MO 63150-3284.
Building Science Series–Disseminates technical information developed at the Institute on building materials, components, systems, and whole structures. The series presents research results, test methods, and performance criteria related to the structural and environmental functions and the durability and safety characteristics of building elements and systems.
Technical Notes–Studies or reports which are complete in themselves but restrictive in their treatment of a subject. Analogous to monographs but not so comprehensive in scope or definitive in treatment of the subject area. Often serve as a vehicle for final reports of work performed at NIST under the sponsorship of other government agencies.
Voluntary Product Standards–Developed under procedures published by the Department of Commerce in Part 10, Title 15, of the Code of Federal Regulations. The standards establish nationally recognized requirements for products, and provide all concerned interests with a basis for common understanding of the characteristics of the products. NIST administers this program in support of the efforts of private-sector standardizing organizations.

Order the following NIST publications–FIPS and NISTIRs–from the National Technical Information Service, Springfield, VA 22161.

Federal Information Processing Standards Publications (FIPS PUB)–Publications in this series collectively constitute the Federal Information Processing Standards Register. The Register serves as the official source of information in the Federal Government regarding standards issued by NIST pursuant to the Federal Property and Administrative Services Act of 1949 as amended, Public Law 89-306 (79 Stat. 1127), and as implemented by Executive Order 11717 (38 FR 12315, dated May 11,1973) and Part 6 of Title 15 CFR (Code of Federal Regulations).
NIST Interagency or Internal Reports (NISTIR)–The series includes interim or final reports on work performed by NIST for outside sponsors (both government and nongovernment). In general, initial distribution is handled by the sponsor; public distribution is handled by sales through the National Technical Information Service, Springfield, VA 22161, in hard copy, electronic media, or microfiche form. NISTIR's may also report results of NIST projects of transitory or limited interest, including those that will be published subsequently in more comprehensive form.

U.S. Department of Commerce
National Institute of Standards and Technology
325 Broadway
Boulder, CO 80305-3337